Environmental Pollution 158 (2010) 3392–3400

Contents lists available at ScienceDirect

Environmental Pollution

journal homepage: www.elsevier.com/locate/envpol

Impact of anthropogenic emissions and open biomass burning on regional carbonaceous aerosols in South China

Gan Zhang [a,*], Jun Li [a], Xiang-Dong Li [b], Yue Xu [a], Ling-Li Guo [a], Jian-Hui Tang [c], Celine S.L. Lee [b], Xiang Liu [a], Ying-Jun Chen [c]

[a] State Key Laboratory of Organic Geochemistry, Guangzhou Institute of Geochemistry, Chinese Academy of Sciences, Guangzhou 510640, China
[b] Department of Civil and Structural Engineering, The Hong Kong Polytechnic University, Hung Hom, Kowloon, Hong Kong
[c] Yantai Institute of Coastal Zone Research, Chinese Academy of Sciences, Yantai 264003, China

Anthropogenic emissions in China and open biomass burning in the Indo-Myanmar region were the two major potential sources for carbonaceous matters in South China region.

ARTICLE INFO

Article history:
Received 5 May 2010
Received in revised form
18 July 2010
Accepted 24 July 2010

Keywords:
Carbonaceous aerosol
Elemental carbon
Southeast Asia
Potential source contribution function (PSCF)
Open biomass burning

ABSTRACT

Carbonaceous aerosols were studied at three background sites in south and southwest China. Hok Tsui in Hong Kong had the highest concentrations of carbonaceous aerosols (OC = 8.7 ± 4.5 μg/m^3, EC = 2.5 ± 1.9 μg/m^3) among the three sites, and Jianfeng Mountains in Hainan Island (OC = 5.8 ± 2.6 μg/m^3, EC = 0.8 ± 0.4 μg/m^3) and Tengchong mountain over the east edge of the Tibetan Plateau (OC = 4.8 ± 4.0 μg/m^3, EC = 0.5 ± 0.4 μg/m^3) showed similar concentration levels. Distinct seasonal patterns with higher concentrations during the winter, and lower concentrations during the summertime were observed, which may be caused by the changes of the regional emissions, and monsoon effects. The industrial and vehicular emissions in East, Southeast and South China, and the regional open biomass burning in the Indo-Myanmar region of Asia were probably the two major potential sources for carbonaceous matters in this region.

1. Introduction

Carbonaceous aerosols are now of worldwide concern for their direct and indirect effects on the earth's radiative balance (Ramanathan et al., 2001a). Elemental carbon (EC, or black carbon, BC) and organic carbon (OC) are two main fractions of carbonaceous matters in the air. EC is among the most strongly absorbing substance in the atmosphere (Horvath, 1993; Ramanathan and Carmichael, 2008), which can cause the heating of elevated aerosol layers, and the inhibition of rainfall. On the contrary, OC has the potential to scatter light directly (Ramanathan et al., 2001a). It has been suggested that hydrophobic organic films could slow or stop the activation of aerosols to form cloud droplets, thus altering the indirect effect of aerosols on climate (Facchini et al., 1999). Therefore, the ratio of OC to EC may affect the degree of radiative forcing of the atmosphere (Ramanathan et al., 2001a).

Particulate EC derives from the combustion of fossil fuels, such as coal, gasoline and diesel, and the burning of vegetation and wood, whereas particulate OC originates from anthropogenic and biogenic sources, including primary emissions from incomplete combustion of fossil fuels, conversion from gas to particulate phase, and natural sources, such as pollen, wind-blown soil, and plant waxes (Novakov et al., 1997). Carbonaceous species have attracted special concern in the areas of rapid economic growth and high population density where large amounts of those species are released into the air. For example, the largest total EC and OC emissions occur over China, and the largest OC emissions per unit surface area occur over India (Ramanathan et al., 2007). It was assumed that precipitation trends in China over the past decades, with increased rainfall in the south and drought in the north, might be related to increased EC aerosols (Menon et al., 2002), and the reduction of the crop yields in China was possibly attributed to the degradation of optical depths and visibility caused by carbonaceous aerosols, reducing solar radiation that reaches the earth (Chameides et al., 1999). Meanwhile, carbonaceous particles are persistent and subjected to long-range atmospheric transport, and its black carbon content and large perturbation to the radiative energy budget have significant implications to the regional and global water budget, agriculture and human health (Ramanathan et al., 2007). Several studies have indicated that the carbonaceous species may cause serious health effects. Although EC is generally

* Corresponding author.
E-mail address: zhanggan@gig.ac.cn (G. Zhang).

0269-7491/$ – see front matter © 2010 Elsevier Ltd. All rights reserved.
doi:10.1016/j.envpol.2010.07.036

considered inert, the combustion process results in the EC being coated with organic matter, such as polycyclic aromatic hydrocarbons (PAHs) and their alkylated homologues. In addition, OC often contains many other persistent organic compounds (POPs), which are potential mutagens or carcinogens, and might pose significant human health risks (Schuetzle, 1983). Therefore, in recent decades, carbonaceous aerosols have been studied at a number of locations in China (Davis and Guo, 2000; Cao et al., 2003, 2007; Zhang et al., 2005, 2008; Feng et al., 2006).

At a regional scale, the effects of atmospheric aerosols on air quality and visibility are of great concern. In the past decade, the intensity of the haze reached a maximum over most of the tropical Indian Ocean, South, Southeast and East Asia (Ramanathan et al., 2001b). Based on the findings of an international experiment, Indian Ocean Experiment (INDOEX), conducted during 1998–2000 over the northern Indian Ocean, the haze in this region, also called Atmospheric Brown Cloud (ABC), is a cocktail of aerosol, ash, soot and other particles. One of the important observations of the INDOEX is that black carbon and fly ash constitute significant portions, up to 14% and 6%, respectively, of the aerosol particles over the Indian Ocean. These pollutants are unquestionably of anthropogenic origins, and are caused by bio-fuel combustion and open biomass burning (Ramanathan et al., 2001b). Eastern and Southern China are the important source region of anthropogenic pollutants, whereas Southeast Asia is an important source region of biomass burning emissions (Streets et al., 2003). The trace gases, nonmethane hydrocarbons, and aerosols emitted from those regions not only enhanced the regional contamination levels (Wang et al., 2003; Chan et al., 2006; Tang et al., 2007), but also could rise up to the free troposphere, and transport through the western Pacific and eventually crossed the Pacific Ocean to North America (de Gouw et al., 2004). However, there is only a limited literature elucidating the impact of the anthropogenic emissions and biomass burning on the regional carbonaceous aerosol in Southeast Asia.

In this study, three regional air-monitoring sites (Fig. 1) were chosen to study the carbonaceous aerosol emitted from anthropogenic activities and open biomass burning in China and Southeast Asia. According to the data of atmospheric monitoring work (Wang et al., 2003; Chan et al., 2006; Tang et al., 2007, 2009), the three sampling sites were subject to the alteration of winds over Asian monsoon, and the temporal and spatial variations of regional industrial emissions and biomass burning (http://maps.geog.umd.edu/products.asp). The present study is therefore essential to evaluate the contribution of anthropogenic activities and open biomass burning to the regional carbonaceous aerosol concentrations and compositions. The sampling strategy at high-altitude background sites is considered to be advantageous for studies on the long-range transport of atmospheric chemical species at a regional scale.

2. Materials and methods

2.1. Site description and regional emission sources

Hok Tsui (HT, D' Aguilar Peak) is located in the southeastern tip of Hong Kong Island (22°12′N, 114°15′E, with an elevation of 60 m above sea level (ASL)). The site is in a relatively clean area of Hong Kong. The sampling location is situated on a coastal cliff with 240 degrees of ocean view stretching from northeast to southwest. Urban areas in Hong Kong (population: 7.1 millions) are normally at downwind area of this site under the prevailing northeasterly and easterly winds. Besides the urban areas of Hong Kong, the regional emissions are concentrated in the Pearl River Delta (PRD) region, north and northwest of Hong Kong. The PRD is one of the most economically developed regions in China. The island of Taiwan is about 600 km east of Hong Kong. Under the prevailing easterly and northeasterly winds, the levels of pollutants at this study site are expected to be largely determined by the transport of air masses from rural areas in South China, the island of Taiwan, high-emission areas in eastern coastal regions of China, and northeast Asia.

Jianfeng (JF) Mountain (18°40′N, 108°49′E, 820 m ASL) is situated at the southwest corner of Hainan Island, South China, and is regarded as a remote background site. It is about 20 km from the coast of Beibu Gulf (Gulf of Tonkin) to the west; 120 km from Sanya, the second largest city of Hainan Province, to the southeast; and 315 km from Haikou, the capital city of Hainan Province, to the northeast. The site faces mountain ranges in the north and east. This sampling site is surrounded by a tropical rainforest with a total area of 475 km^2. The air sampling station is located at a National Field Monitoring Station for the tropical rainforest. Air samples were collected on the rooftop of a two-story building at this station. There are several hills around the sampling site with elevation above 1000 m. Anthropogenic emissions transported from the Southeast and South China, and biomass burning from Southeast Asia were probably the two major potential sources at this site (Tang et al., 2007).

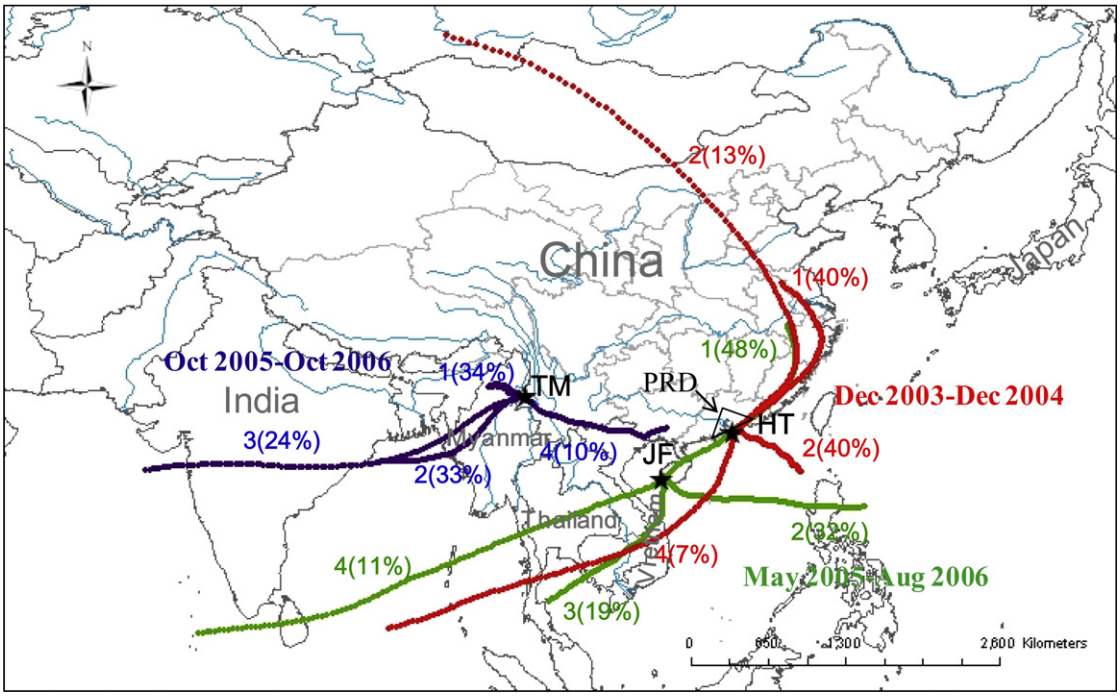

Fig. 1. Typical wind directions during the sampling times at the three sites. Numbers present the trajectory types, and the numbers (%) present the percentage of the trajectories that occurred in a whole year.

Tengchong Mountain (TM) (24°57′N, 98°29′E, 1960 m ASL) is a remote site on the eastern border between Yunnan Province and Myanmar (about 60 km to the east of the Myanmar), and 750 km to the west of Kunming (with an urban population of 3 millions in 225 km^2 area), the capital city of Yunnan Province. The closest town, Tengyue is about 10 km to the south. There are several small villages surrounding the sampling site. Air samples were collected on the mountaintop within Tengchong observatory station, which is one of the stations of the Global Climate Observing System (GCOS), WMO. The potential pollutants to this sampling location are regional bio-fuel combustions and biomass burning emissions transported from Southeast Asia (Chan et al., 2006; Tang et al., 2009).

2.2. Sampling procedure

The aerosol samples were collected using high-volume samplers, operated at a flow rate of 0.22–0.34 m^3/min for about 24 h in order to filter nearly 300 m^3 of air, onto quartz microfiber filters (Whatman, QM-A, 20.3 cm × 25.4 cm, pre-combusted at 450 °C). The filters had a collection efficiency of 99.9% for the particles up to size 0.3 μm. All filters were wrapped in aluminium foil and stored in polyethylene bags. In total, 24 samples were collected (one sample every two weeks) from HT during Dec 2003–Dec 2004; whereas 61 samples (about one sample per week) from JF during May 2005–Aug 2006, and 54 samples (about one sample per week) from TM during Oct 2005–Oct 2006. The filters were weighed using a balance (Sartorius, Analytic) with an accuracy of 0.1 mg after conditioning in an electronic desiccator (RH = 50% and temperature = 25 °C) before and after the sample collection. After weighing, loaded filters were stored in a refrigerator at about −20 °C before chemical analysis to prevent evaporation of volatile components. Also, field blank filters were collected to subtract the possible contamination that occurred during and/or after sampling.

2.3. Thermal-optical carbon analysis

Portions of filter samples (1.5 cm^2) were cut for analyzing organic and elemental carbon contents (OC/EC) by a thermal-optical carbon analyzer (Sunset Laboratory Inc., Forest Grove, OR) with a modified NIOSH (National Institute of Occupational Safety and Health) thermal-optical transmission (TOT) protocol. The punch aliquot of filter was heated stepwise at temperatures of 250 °C, 60 s; 500 °C, 60 s; 650 °C, 60 s; and 850 °C, 90 s in a pure helium atmosphere for detecting the OC fraction, and at temperatures of 550 °C, 45 s; 650 °C, 60 s; 750 °C, 60 s; 850 °C, 40 s; and 870 °C, 40 s in an oxidizing atmosphere of 2% oxygen (by volume) in a balance of helium for detecting the EC fraction. The carbon evolved at each temperature is oxidized to carbon dioxide (CO_2) and then reduced to methane (CH_4) for quantification with a flame ionization detector (FID). Some of OC pyrolyzes to EC as the temperature increases in inert helium, and is subtracted from the elemental carbon area according to the initial laser absorbance. At the end of every analysis, a fixed volume loop of methane is injected automatically as an internal standard to calculate the carbon results (Zhi et al., 2008).

2.4. Quality control

Replicate samples and filter blank were collected to determine analytical precision and background contamination. The replicate analysis of samples ($n = 26$) provided a good analytical precision; with relative deviation of 7.4, 6.9, and 6.9% for OC, EC and TC, respectively. The average field filter blank concentration of OC was 0.19 ± 0.16 μg cm^{-2} (1σ, $n = 15$) while EC signal from the blank filters was undetectable. The OC concentrations have been corrected with the field blank value.

2.5. Air trajectory generation

The hybrid single-particle Lagrangian integrated trajectory (HYSPLIT) model was used to generate backward air mass movement, which is available on the National Oceanic and Atmospheric Administration (NOAA) Air Resource Laboratory website (www.arl.noaa.gov/ready/hysplit4.html). Five-day backward trajectories were generated at four different starting times at 6 h intervals during the 24 h sampling period. In each case, the trajectories were calculated at three different starting altitudes: 100, 500, and 1000 m above ground level. The calculations used the ETA Data Assimilation System database of archived meteorological data.

2.6. Potential source contribution function (PSCF)

To identify the likely source regions of OC and EC at the three sites, potential source contribution function (PSCF) analyses were performed. PSCF has now been applied in a large number of source identification and apportionment studies (Cheng et al., 1993; Zhang et al., 2005). The detailed description of the mathematical structure of PSCF was reported in a previous work (Cheng et al., 1993). The PSCF was calculated using five-day backward trajectories calculated using the HYSPLIT model at a height of 100 m above ground level. The region covered by the trajectories was divided into grid cells of 1° × 1° latitude and longitude. The PSCF value for a single grid cell was calculated by counting each trajectory segment endpoint that terminates within that grid cell. The number of endpoints that fall in the ijth cell is denoted as n_{ij}. The number of endpoints for the same cell having times of arrival at the sampling site corresponding to pollutant concentrations higher than an arbitrarily criterion value is defined to be m_{ij}. The PSCF value for the ijth cell is then defined as:

$$\mathrm{PSCF}_{ij} = m_{ij}/n_{ij} \quad (1)$$

In this study, the criterion value was set to the mean concentration of all OC and EC data. All of these values were plotted vs the cell locations using mapping software (ArcGIS 9.2). Only the cells with at least 10 points or more were plotted.

3. Results and discussion

3.1. Carbonaceous species levels

The summary statistics of the concentrations of total suspended particle (TSP) mass, EC and OC from the three sites were shown in Fig. 2. Among the three sampling sites, HT had the highest concentrations of TSP mass, OC and EC, ranged from 45.9 to 376 μg/m^3, 2.6 to 17.7 μg/m^3, and 0.3 to 6.6 μg/m^3, respectively. The average concentrations of OC and EC at HT were 8.7 ± 4.5 and 2.5 ± 1.9 μg/m^3, respectively, which accounted for 5.3 ± 2.3% and 1.4 ± 1.0% of the TSP. The high values at HT could be attributed to the anthropogenic emission sources from the Pearl River Delta (PRD) and the Southeast China coastal areas (So et al., 2007). At this sampling site, only carbonaceous matters in $PM_{2.5}$ and PM_{10} have been studied previously (Ho et al., 2003; So et al., 2007). However, the concentrations of carbonaceous particles in this study were similar to the reported values in $PM_{2.5}$ at this site during Nov 2000 to Feb 2001 (5.52 ± 1.13 μg/m^3 for OC and 1.36 ± 0.40 μg/m^3 for EC) (Ho et al., 2003), and the results in $PM_{2.5}$ during 2004/2005 year (4.25 μg/m^3 for OC and 2.14 μg/m^3 for EC) (So et al., 2007). The carbonaceous matter at this location was predominantly associated with fine airborne particles (Ho et al., 2003). In comparison with other recent studies in China, the OC and EC concentrations were similar to the reported values at Changdao, an island at the demarcation line of Bohai Sea and Yellow Sea, and along the path of the Asian continental outflow (Feng et al., 2007), and at the low end of the concentration range for some rural sites (with ranges of 11–30 μg/m^3 and 2–5 μg/m^3 for OC and EC, respectively) in China (Zhang et al., 2008).

TSP, OC and EC abundances from other two remote background sites were similar (Fig. 2.) The TSP, OC and EC abundances ranged from 3.5 to 88.3 μg/m^3 (Av: 47.0 ± 20.6 μg/m^3, $n = 60$, excluding one value of 103.0 μg/m^3, the values above 90th or below 10th percentiles were excluded), 1.5 to 12.5 μg/m^3 (Av: 5.8 ± 2.6 μg/m^3, $n = 59$, excluding two values of 14.4 and 13.5 μg/m^3), and 0.2 to 2.0 μg/m^3 (Av: 0.8 ± 0.4 μg/m^3, $n = 60$, excluding one value of 2.4 μg/m^3), respectively, at the JF site, whereas those at the TM site ranged from 17.5 to 171 μg/m^3 (Av: 55.6 ± 41.0 μg/m^3, $n = 51$, excluding three values of 318, 234 and 220 μg/m^3), 0.9 to 15.5 μg/m^3 (Av: 4.8 ± 4.0 μg/m^3, $n = 53$, excluding one value of 33.8 μg/m^3), and 0.04 to 1.4 μg/m^3 (Av: 0.5 ± 0.4 μg/m^3, $n = 53$, excluding one value of 2.4 μg/m^3), respectively. On the average, OC and EC at JF accounted for 16.0 ± 10.9% and 2.2 ± 1.5% of the TSP, respectively. In contrast, OC and EC at TM accounted for 8.9 ± 4.9% and 0.9 ± 0.5% of the TSP. These OC and EC concentrations were similar to those values measured at other CAWNET (China Atmosphere Watch Network) remote background stations, such as at Mt. Waliguan (EC values of 0.13–0.30 μg/m^3) (Tang et al., 1999), Shangri-La, Zhuzhang (OC and EC averaged 3.1 ± 0.91 and 0.34 ± 0.18, respectively), and Akdala (OC and EC averaged 2.8 ± 1.2 and 0.36 ± 0.31, respectively) (Zhang et al., 2008), and were also comparable to those measured at other remote sites in the world, such as at the high-altitude sites (Mt. Abu) in India with annual-average abundances of OC and EC values of 3.7 ± 2.4 μg/m^3 and 0.5 ± 0.5 μg/m^3, respectively (Ram et al., 2008), at the S. Pietro Capofiume in Europe (EC mean of 0.53 μg/m^3) (Decesari et al., 2001), and at the Galveston background site in North America (EC mean of 0.8 μg/m^3) (Fraser et al., 2002). These comparisons

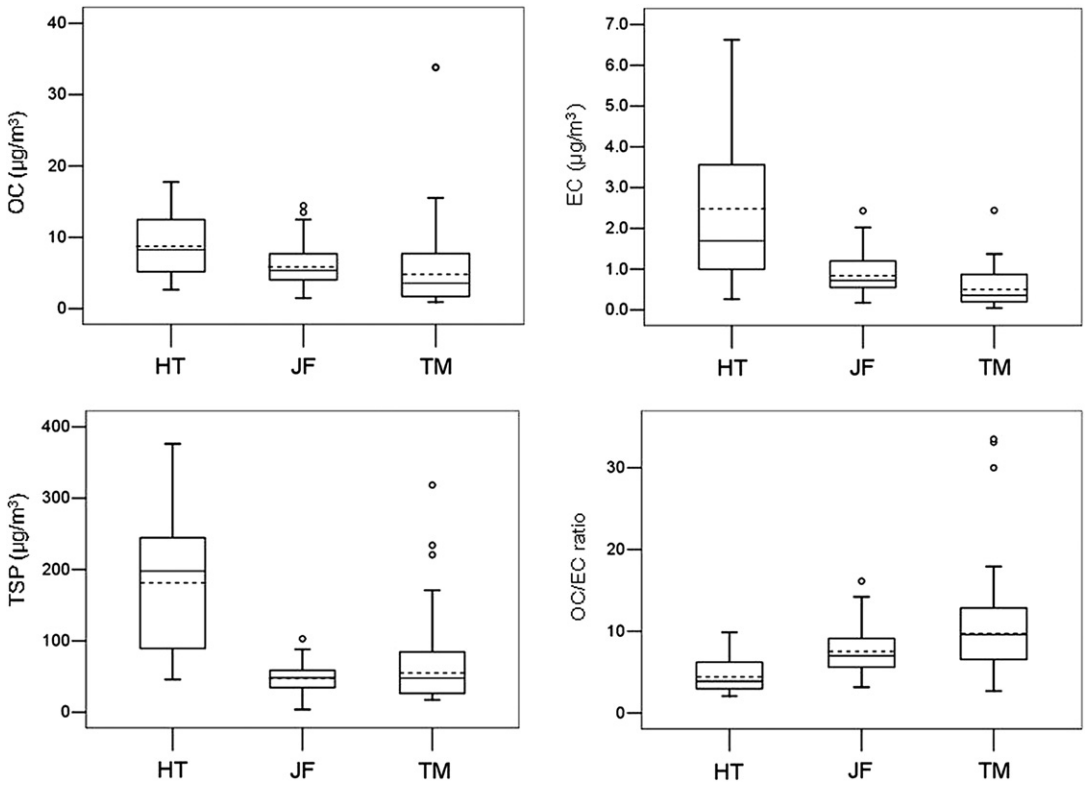

Fig. 2. Box plots of OC, EC, TSP and OC/EC ratios at the three sampling sites. The boundary of the box closest to zero indicates the 25th percentile, a line within the box marks the median, and the boundary of the box farthest from zero indicates the 75th percentile. Whiskers (error bars) above and below the box indicate the 90th and 10th percentiles. The mean is represented by a dashed line and points lying outside the whiskers denote the outliers.

suggested that the background air in south and southwest China was relatively less influenced by anthropogenic emissions than that in east and southeast regions of China.

3.2. Seasonal trends of carbonaceous materials

3.2.1. HT

The concentrations of OC and EC at the HT site showed strong seasonal variations with high concentrations in the winter, and low concentrations in the summer (Fig. 3). Topographic features and Asian monsoon make this sampling site a receptor of large amounts of pollutant emissions in the East Asian Pacific Rim (Chan and Chan, 2000; Lee et al., 2007; Li et al., 2007). The 5-day back trajectory analysis showed the seasonal variations of carbonaceous materials were consistent with the change of the winter and summer monsoons. The relatively higher concentrations of OC and EC were observed when the air masses were continental in nature from the mainland China flowing southwards to reach the site during the Asian winter monsoon season. For example, elevated OC and EC concentrations were observed on 31st December 2003 and 24th August 2004 at HT (see Fig. 3). On these episodic days, the concentrations of OC and EC on 31st Dec 2003 attained high concentrations of 14.5 and 6.6 μg/m^3, respectively, and those measured on 24th Aug 2004 reached 13.1 and 6.3 μg/m^3, respectively. The back trajectory analysis (not shown here) indicated that the air mass originated from Eurasia, and traveled southwards through continental inland areas of China to the coastal area of Hong Kong. Subsequently, the air masses passed through the PRD region at a moderate speed before reaching Hong Kong via northerly winds (Lee et al., 2007).

The OC/EC ratio can be used to determine the possible influences of anthropogenic activities on aerosol composition. A low OC/EC ratio generally indicates anthropogenic influences on aerosol composition due to the larger fraction of combustion derived elemental carbon (Turpin and Huntzicker, 1991). In the special episodic date, the OC/EC ratios of the carbonaceous matters were low with the values of 2.2 and 2.1, respectively, which were similar to that of industrial and vehicular emissions. Meanwhile, the hypothesis was also supported by the fact that the heavy metal compositions and the Pb isotopic ratios of the aerosols closely resembled those of the Pb ore and industrial and vehicular emissions sources in the PRD region (Lee et al., 2007). Anthropogenic emissions in the northern inland areas of China and the PRD region could contribute to the enrichment of carbonaceous aerosols in the downwind areas of Hong Kong through the long-range transport of air pollutants. On the contrary, during the summer monsoon season, when the air masses originated from the middle Pacific or the South China Sea (air trajectories not shown), the lower OC and EC concentrations were observed, such as the two typical days, 12th May 2004 and 7th July 2004. The trajectory on 12th May 2004 showed that the air mass originated from the Philippines traveling north-westerly, which eventually reached the coastal areas of South China region. On the other hand, the air mass on 7th July 2004 originated from the Indian Ocean, and moved in a northeasterly direction, passing through the South Asian countries, such as Vietnam and Malaysia, to the coastal areas of South China region. Moreover, the Pb isotopic ratios of those aerosols were similar to those of South Asian aerosols (Lee et al., 2007). Thus, the levels of EC monitored during this season also reflected the regional background levels of elemental carbon in the South Asia region. Compared with the aerosols during the winter monsoon season, the OC/EC ratios of the corresponding samples were high with the values of 9.9 and 4.8, respectively. The higher OC/EC ratios can be attributable to the predominance of organic carbon, mainly derived from biomass burning sources along with the secondary organic carbon (SOC). For example, previous studies

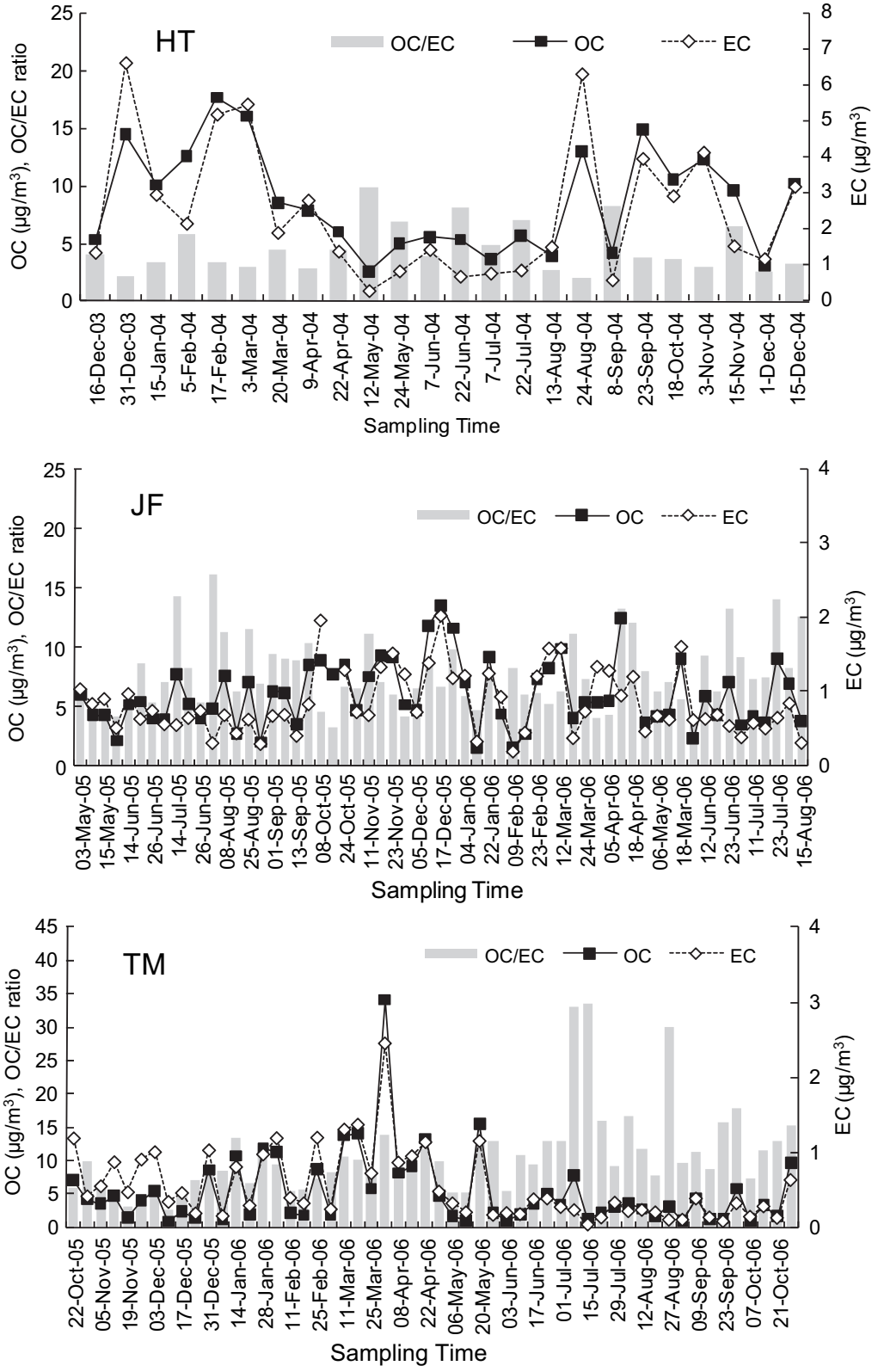

Fig. 3. Temporal variations of OC, EC abundances (μg/m^3) with the OC/EC ratios at the three sites.

reported that OC/EC ratios were as high as 16.8–40.0 for residential wood burning, and 7.7 for biomass burning (Zhang et al., 2007). In addition, the formation of the SOC might be another source for the enhancement of the organic carbon (Chow et al., 1993).

3.2.2. JF and TM

The OC and EC concentrations of aerosols measured at these two remote sites (JF and TM) over one-year period are plotted as a time-series pattern in Fig. 3. Distinguished seasonal patterns were also found in the EC concentrations of aerosols at both sampling sites. The lower and relatively consistent values were obtained in the summer/rainy season, from late May to September, and higher and significant varied values occurred in late autumn, winter and spring, from October to early May. Particulate EC predominantly derives from the combustion of fossil fuels, such as coal, gasoline and diesel, and burning of vegetation and wood. The seasonal characteristics of EC concentrations at the remote sites can be explained as the combined impact of climatic conditions and regional pollutant emissions. During the summer monsoon seasons, *i.e.*, usually from May to September, air masses were originated from the marine areas together with abundant precipitation. The back trajectory showed that, at the JF site, the air masses originated from Indian Ocean or South China Sea, and passed over the SE Asian continent or from the western Pacific and the South China Sea; and at the TM site, the air masses originated from the Bay of Bengal and its surrounding regions, and traveled across Myanmar and sometimes the Myanmar–Bangladesh and Bhutan border and less frequently the northern part of Thailand and Laos. Moreover, during these seasons, the fire counts map showed the biomass burning activities in Southeast Asia was relatively minor. The fire counts were detected by MODIS (Moderate Resolution Imaging Spectroradiometer) on the NASA satellites and the integrated data are available at the website of the University of Maryland (http://maps.geog.umd.edu/products.asp). One fire point in the map represents an active fire in a 1×1 km pixel. During the other times, the Southeast Asia is controlled by the winter monsoon with air masses originated from the Asia continent. The climate is generally dry during the winter season. Not only were the greater amounts of EC emitted from the human activities in the important habitat areas (Cao et al., 2007; Zhang et al., 2008), but also large amounts of this pollutant would be generated from the open biomass burning in Southeast Asia (Tang et al., 2007). Notable exceptions occur in other seasons between the two sampling sites with different monthly maxima. At the JF site, the highest concentration of EC was observed from October 2005 to April 2006, whereas, at the TM site, the highest level of EC value was monitored from March 2006 to April 2006. This seasonal difference of EC maxima concentrations between the two remote sites could be elucidated by the impact of the upwind emission sources on the receptor. The trajectory from October to December 2005 showed that the air masses passed through different areas before reaching the two sampling sites. For examples, the air mass predominantly originated from the boundary layer of mainland China and East Asia, passed over the coast of southeast and south China, and then reached the JF site. Whereas, the air masses predominantly originated from the coast of southeast China and the South China Sea, traveled across the northern part of Vietnam, Laos and Myanmar and ended at the TM site. Meanwhile, during the sampling times, intensive biomass burning activities occurred in South China. Fig. 4 shows the backward trajectory of the corresponding days in October at two sampling sites (Fig. 4B), and the fire count map on October 2005 for the SE Asian region (Fig. 4A). Elevated EC concentrations were observed on 8th, 17th, and 24th October 2005 at JF with the values of 2.0, 2.4 and

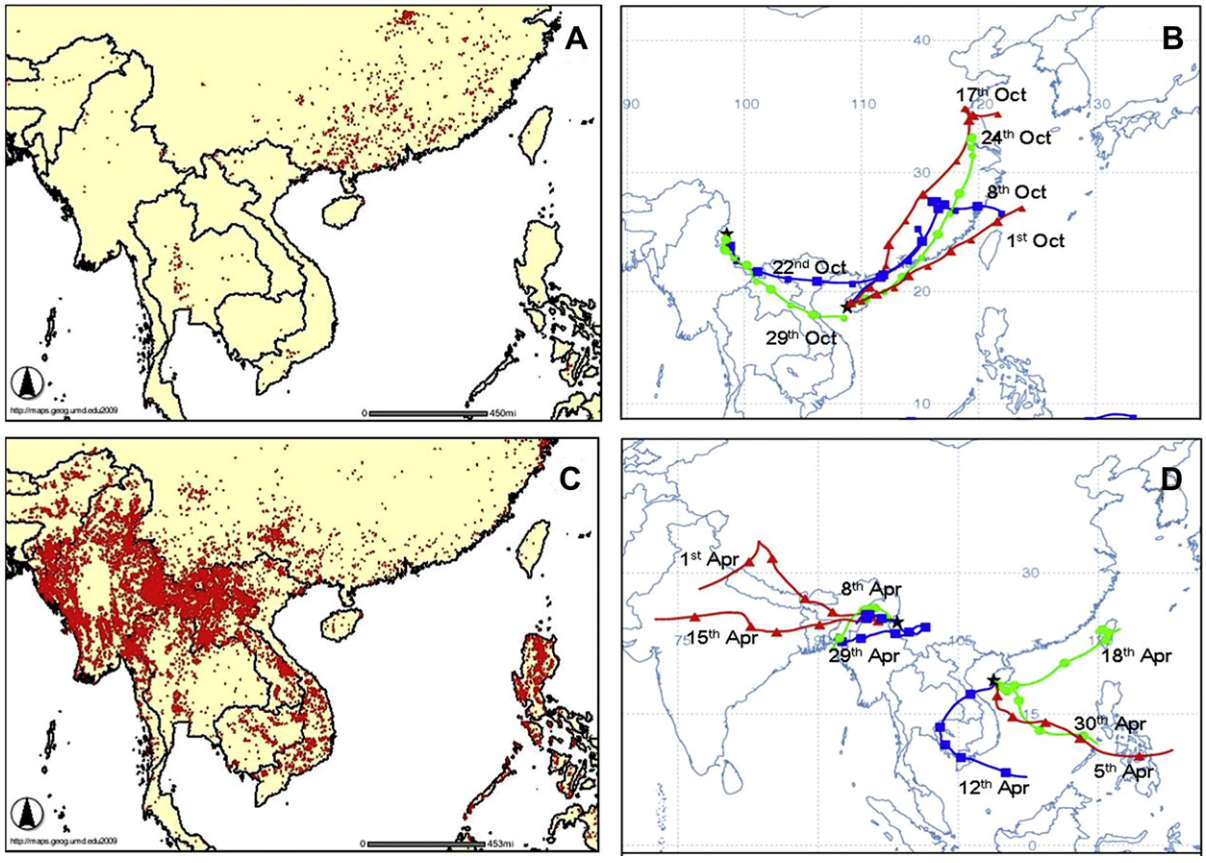

Fig. 4. Fire count map in October 2005 (A) and April 2006 (C), back trajectories in October 2005 (B) and April 2006 (D) at the JF and TM sites.

1.3 μg/m^3, respectively (Fig. 3JF), when the air mass passed through South China region near the Pearl River Delta (PRD). High levels of EC concentrations from vehicle emission and fossil fuels combustion were monitored in this region in previous studies (Cao et al., 2003; Zhang et al., 2008). The OC/EC ratios of those aerosol samples were relatively low. The mixing of industrial and vehicular emissions and open biomass burning in southern inland areas of China and the PRD region could contribute to the enrichment of EC in the remote areas of Jianfeng Mountain through the long-range transport of air pollutants. A similar phenomenon was also observed on the 22nd October 2005 at the TM site (Fig. 3TM). The trajectories showed that the air mass originated from the south China near the PRD region, and passed through the northern part of Vietnam and Laos (Fig. 4B). On the contrary, from March to April 2006, the regions of biomass burning activities and the routes of air masses all changed. Fig. 4 also shows the fire count maps in April 2006 in Southeast Asian region (Fig. 4C), and the back trajectory of the corresponding sampling days at the both remote sampling sites (Fig. 4D). In April, intensive biomass burning activities were detected at the Southeast Asian subcontinent. TM site is in the proximity of the biomass burning areas and mainly influenced by air mass from this region. Consequently, the highest concentrations of EC were observed at this site (Fig. 3). Based on the observation of ozone, trace gases and aerosols at the same site in the Spring 2004, the pollutant levels in this relatively undeveloped region of Southwest China were mainly impacted by the biomass-burning emissions associated with fire activities in the SE Asian subcontinent (Chan et al., 2006). JF site is relatively isolated from the open burning source during the same times, but the higher concentrations of EC were still observed when the air masses passed through the Southeast Asian region (Fig. 4C, D).

Less temporal variability was found in the OC concentrations of aerosols at the JF site, while particulate OC concentrations at the TM site displayed a clearly seasonal trend similar to EC (see Fig. 3). Particulate OC not only originates from combustion emissions, but also from the formation of SOC and natural sources, such as pollen, wind-blown soil, and plant waxes (Novakov et al., 1997). Generally, OC-EC relationship and OC/EC ratios can give some indication of the origins of carbonaceous particles. Strong relationship between OC and EC might elucidate the carbonaceous particles derived from the same emission source. Lower values of the OC/EC ratio (OC/EC = 1.0–4.2) may imply the sources from diesel- and gasoline-powered vehicular exhaust (Schauer et al., 1999, 2002), while higher OC/EC ratios of aerosols might source from wood combustion (16.8–40.0) (Schauer et al., 2001), forest fires (14.5), biomass burning (7.7) (Zhang et al., 2007), and formation of second organic aerosol (SOA) (Chow et al., 1993). At the two sites, the correlations

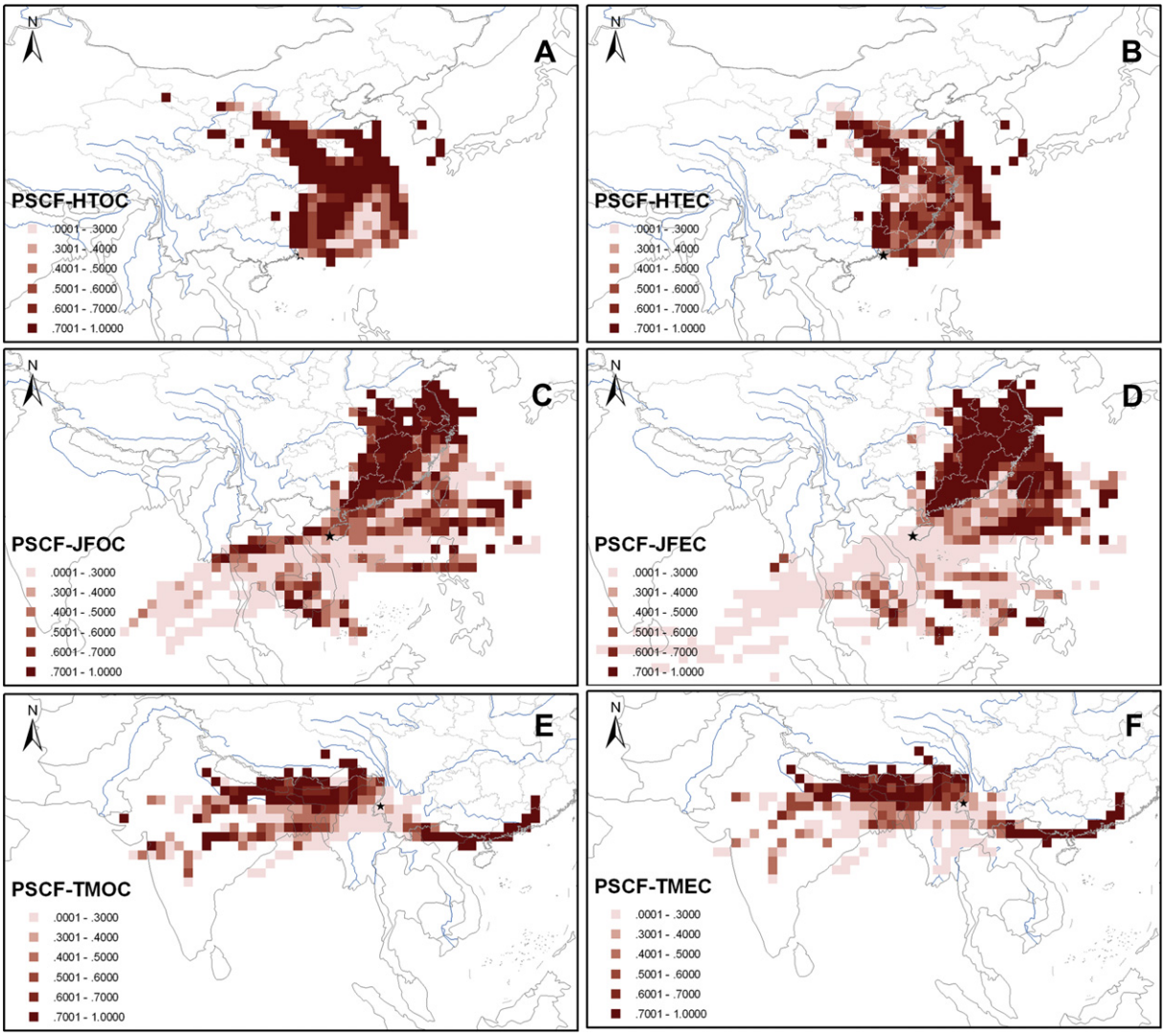

Fig. 5. Potential source contribution function (PSCF) results of OC and EC for HT (A and B), JF (C and D), and TM (E and F) samples.

between OC and EC ($R^2 = 0.43$, excluding two samples at JF, $R^2 = 0.74$, excluding one sample at TM) were lower than that of aerosols from common emission sources in cities (Cao et al., 2003). The statistical median values of the OC/EC ratios in aerosols at JF and TM sites were 7.0 (range from 2.9 to 16.1, mean value of 7.7 ± 2.9), and 9.6 (range from 2.7 to 33.5, mean value of 10.8 ± 6.4), respectively, which may indicate that the carbonaceous aerosols were probably derived from the mixture of various sources.

3.3. Sources of OC and EC using the PSCF model

Maps of potential OC and EC source regions for the three sampling sites are shown in Fig. 5. Since the plotted cells must meet the criteria of 10 or more hourly points, some potential source regions could be excluded in the maps. At the coastal site of the South China – HT, the PSCF results for OC (Fig. 5A) and EC (Fig. 5B) were similar. The maps also indicated that the major source areas of the carbonaceous aerosols were the more developed region of China, including some parts of the central China, east, southeast and south China. Besides those areas, Taiwan, south of Korea and west of Japan were also the potential source regions.

The major pollution source areas (east, southeast and south China) for JF were similar to those for HT (Fig. 5C and D), suggesting intensive impact of atmospheric pollutants to Hainan Island of South China from the most industrialized and urbanized regions of China. Due to the location, several Southeast Asian countries were also the potential source regions of carbonaceous matters, especially for the OC at JF, which might be attributed to the open biomass burning.

For TM site, South China was still a major source region for OC and EC, and another major source may come from the Indo-Myanmar region of northern Southeast Asia subcontinent, including northeast India, Bangladesh, and northern Myanmar (Fig. 5E and F).

4. Conclusion

The concentrations of OC and EC varied greatly among the three background sites. HT, the coastal site closed to the most industrialized and urbanized region in south China, had the highest concentrations of carbonaceous aerosols, which were at the low end of the value reported for the rural sites in China; and the JF and TM sites showed the similar levels of OC and EC, which were comparable to those measured at other CAWNET remote background stations in China. Distinct seasonal trends were found in the OC and EC concentrations of aerosols at the three sites, with higher concentrations recorded during the winter monsoon period, and lower concentrations during the summertime. Combining the back trajectory analysis and fire count maps, the seasonal concentrations of carbonaceous materials in this region reflected the seasonal emissions from anthropogenic activities and open biomass burning, and the alternation of monsoon direction. At HT site, the carbonaceous aerosols mainly come from industrial and vehicular emissions, while at other two remote sites, large portions of those pollutants came from the regional open biomass burning. The maps of the potential source regions illustrated the fast industrialized and urbanized regions in east, southeast and south China were the major source regions of OC and EC, and another potential source areas was the Indo-Myanmar region of northern Southeast Asia subcontinent, especially for the JM and TM sites. In the future, carbon isotope signature of carbonaceous aerosols might be another supplementary tool to apportion the sources of OC and EC in the environmental samples.

Acknowledgements

This work was supported by the Innovative Program of the Chinese Academy of Sciences (KZCX2-YW-GJ02), the Natural Science Foundation of China (NSFC) (no. 40739001 and 40518002), the Earmarked Fund of the State Key Laboratory of Organic Geochemistry (SKLOG2008a04), and the Research Grants Council (RGC) of the Hong Kong SAR Government (PolyU 5147/03E and N_PolyU535/05). This is contribution No. IS-1234 from GIGCAS.

References

Cao, J.J., Lee, S.C., Chow, J.C., Watson, J.G., Ho, K.F., Zhang, R.J., Jin, Z.D., Shen, Z.X., Chen, G.C., Kang, Y.M., Zou, S.C., Zhang, L.Z., Qi, S.H., Dai, M.H., Cheng, Y., Hu, K., 2007. Spatial and seasonal distributions of carbonaceous aerosols over China. J. Geophys. Res. Atmos. 112, D22S11.

Cao, J.J., Lee, S.C., Ho, K.F., Zhang, X.Y., Zou, S.C., Fung, K., Chow, J.C., Watson, J.G., 2003. Characteristics of carbonaceous aerosol in Pearl River Delta Region, China during 2001 winter period. Atmos. Environ. 37, 1451–1460.

Chameides, W.L., Yu, H., Liu, S.C., Bergin, M., Zhou, X., Mearns, L., Wang, G., Kiang, C.S., Saylor, R.D., Luo, C., Huang, Y., Steiner, A., Giorgi, F., 1999. Case study of the effects of atmospheric aerosols and regional haze on agriculture: an opportunity to enhance crop yields in China through emission controls? Proc. Natl. Acad. Sci. U.S.A. 96, 13626–13633.

Chan, C.Y., Chan, L.Y., 2000. Effect of meteorology and air pollutant transport on ozone episodes at a subtropical coastal Asian city, Hong Kong. J. Geophys. Res. Atmos. 105, 20707–20724.

Chan, C.Y., Wong, K.H., Li, Y.S., Chan, L.Y., Zheng, X.D., 2006. The effects of Southeast Asia fire activities on tropospheric ozone, trace gases and aerosols at a remote site over the Tibetan Plateau of Southwest China. Tellus Ser. B – Chem. Phys. Meteorol. 58, 310–318.

Cheng, M.D., Hopke, P.K., Barrie, L., Rippe, A., Olson, M., Landsberger, S., 1993. Qualitative determination of source regions of aerosol in Canadian high arctic. Environ. Sci. Technol. 27, 2063–2071.

Chow, J.C., Watson, J.G., Pritchett, L.C., Pierson, W.R., Frazier, C.A., Purcell, R.G., 1993. The dri thermal optical reflectance carbon analysis system – description, evaluation and applications in United-States air-quality studies. Atmos. Environ. Part A – Gen. Topics 27, 1185–1201.

Davis, B.L., Guo, J.X., 2000. Airborne particulate study in five cities of China. Atmos. Environ. 34, 2703–2711.

de Gouw, J.A., Cooper, O.R., Warneke, C., Hudson, P.K., Fehsenfeld, F.C., Holloway, J.S., Hubler, G., Nicks, D.K., Nowak, J.B., Parrish, D.D., Ryerson, T.B., Atlas, E.L., Donnelly, S.G., Schauffler, S.M., Stroud, V., Johnson, K., Carmichael, G.R., Streets, D.G., 2004. Chemical composition of air masses transported from Asia to the U.S. west coast during ITCT 2K2: fossil fuel combustion versus biomass-burning signatures. J. Geophys. Res. Atmos. 109, D23S20.

Decesari, S., Facchini, M.C., Matta, E., Lettini, F., Mircea, M., Fuzzi, S., Tagliavini, E., Putaud, J.P., 2001. Chemical features and seasonal variation of fine aerosol water-soluble organic compounds in the Po Valley, Italy. Atmos. Environ 35, 3691–3699.

Facchini, M.C., Mircea, M., Fuzzi, S., Charlson, R.J., 1999. Cloud albedo enhancement by surface-active organic solutes in growing droplets. Nature 401, 257–259.

Feng, J.L., Guo, Z.G., Chan, C.K., Fang, M., 2007. Properties of organic matter in PM2.5 at Changdao Island, China – a rural site in the transport path of the Asian continental outflow. Atmos. Environ. 41, 1924–1935.

Feng, J.L., Hu, M., Chan, C.K., Lau, P.S., Fang, M., He, L.Y., Tang, X.Y., 2006. A comparative study of the organic matter in PM2.5 from three Chinese mega-cities in three different climatic zones. Atmos. Environ. 40, 3983–3994.

Fraser, M.P., Yue, Z.W., Tropp, R.J., Kohl, S.D., Chow, J.C., 2002. Molecular composition of organic fine particulate matter in Houston, TX. Atmos. Environ. 36, 5751–5758.

Ho, K.F., Lee, S.C., Chan, C.K., Yu, J.C., Chow, J.C., Yao, X.H., 2003. Characterization of chemical species in PM2.5 and PM10 aerosols in Hong Kong. Atmos. Environ. 37, 31–39.

Horvath, H., 1993. Atmospheric light-absorption – a review. Atmos. Environ. Part A – Gen. Topics 27, 293–317.

Lee, C.S.L., Li, X.D., Zhang, G., Li, J., Ding, A.J., Wang, T., 2007. Heavy metals and Pb isotopic composition of aerosols in urban and suburban areas of Hong Kong and Guangzhou, South China – evidence of the long-range transport of air contaminants. Atmos. Environ. 41, 432–447.

Li, J., Zhang, G., Guo, L.L., Xu, W.H., Li, X.D., Lee, C.S.L., Ding, A.J., Wang, T., 2007. Organochlorine pesticides in the atmosphere of Guangzhou and Hong Kong: regional sources and long-range atmospheric transport. Atmos. Environ. 41, 3889–3903.

Menon, S., Hansen, J., Nazarenko, L., Luo, Y.F., 2002. Climate effects of black carbon aerosols in China and India. Science 297, 2250–2253.

Novakov, T., Hegg, D.A., Hobbs, P.V., 1997. Airborne measurements of carbonaceous aerosols on the East Coast of the United States. J. Geophys. Res. Atmos. 102, 30023–30030.

Ram, K., Sarin, M.M., Hegde, P., 2008. Atmospheric abundances of primary and secondary carbonaceous species at two high-altitude sites in India: sources and temporal variability. Atmos. Environ. 42, 6785–6796.

Ramanathan, V., Carmichael, G., 2008. Global and regional climate changes due to black carbon. Nat. Geosci. 1, 221–227.

Ramanathan, V., Crutzen, P.J., Kiehl, J.T., Rosenfeld, D., 2001a. Atmosphere – aerosols, climate, and the hydrological cycle. Science 294, 2119–2124.

Ramanathan, V., Crutzen, P.J., Lelieveld, J., Mitra, A.P., Althausen, D., Anderson, J., Andreae, M.O., Cantrell, W., Cass, G.R., Chung, C.E., Clarke, A.D., Coakley, J.A., Collins, W.D., Conant, W.C., Dulac, F., Heintzenberg, J., Heymsfield, A.J.,

Holben, B., Howell, S., Hudson, J., Jayaraman, A., Kiehl, J.T., Krishnamurti, T.N., Lubin, D., McFarquhar, G., Novakov, T., Ogren, J.A., Podgorny, I.A., Prather, K., Priestley, K., Prospero, J.M., Quinn, P.K., Rajeev, K., Rasch, P., Rupert, S., Sadourny, R., Satheesh, S.K., Shaw, G.E., Sheridan, P., Valero, F.P.J., 2001b. Indian Ocean experiment: an integrated analysis of the climate forcing and effects of the great Indo-Asian haze. J. Geophys. Res. Atmos. 106, 28371–28398.

Ramanathan, V., Li, F., Ramana, M.V., Praveen, P.S., Kim, D., Corrigan, C.E., Nguyen, H., Stone, E.A., Schauer, J.J., Carmichael, G.R., Adhikary, B., Yoon, S.C., 2007. Atmospheric brown clouds: hemispherical and regional variations in long-range transport, absorption, and radiative forcing. J. Geophys. Res. Atmos. 112, D22S21.

Schauer, J.J., Kleeman, M.J., Cass, G.R., Simoneit, B.R.T., 1999. Measurement of emissions from air pollution sources. 2. C_1 through C_{30} organic compounds from medium duty diesel trucks. Environ. Sci. Technol. 33, 1578–1587.

Schauer, J.J., Kleeman, M.J., Cass, G.R., Simoneit, B.R.T., 2001. Measurement of Emissions from air pollution sources. 3. C_1–C_{29} organic compounds from fireplace combustion of wood. Environ. Sci. Technol. 35, 1716–1728.

Schauer, J.J., Kleeman, M.J., Cass, G.R., Simoneit, B.R.T., 2002. Measurement of emissions from air pollution sources. 5. C_1–C_{32} organic compounds from gasoline-powered motor vehicles. Environ. Sci. Technol. 36, 1169–1180.

Schuetzle, D., 1983. Sampling of vehicle emissions for chemical-analysis and biological testing. Environ. Health Perspect. 47, 65–80.

So, K.L., Guo, H., Li, Y.S., 2007. Long-term variation of PM2.5 levels and composition at rural, urban, and roadside sites in Hong Kong: increasing impact of regional air pollution. Atmos. Environ. 41, 9427–9434.

Streets, D.G., Yarber, K.F., Woo, J.H., Carmichael, G.R., 2003. Biomass burning in Asia: annual and seasonal estimates and atmospheric emissions. Global Biogeochem. Cycles 17.

Tang, J., Wen, Y., Zhou, L., Neil, T., Erika, W., 1999. Observational study of black carbon in clean air area of Western China. Quart. J. Appl. Meteorol. 10, 164–170 (in Chinese).

Tang, J.H., Chan, L.Y., Chan, C.Y., Li, Y.S., Chang, C.C., Liu, S.C., Li, Y.D., 2007. Non-methane hydrocarbons in the transported and local air masses at a clean remote site on Hainan Island, south China. J. Geophys. Res. Atmos. 112, D14316.

Tang, J.H., Chan, L.Y., Chang, C.C., Liu, S., Li, Y.S., 2009. Characteristics and sources of non-methane hydrocarbons in background atmospheres of eastern, south-western, and southern China. J. Geophys. Res. Atmos. 114, D03304.

Turpin, B.J., Huntzicker, J.J., 1991. Secondary formation of organic aerosol in the Los Angeles Basin California USA – a descriptive analysis of organic and elemental carbon concentrations. Atmos. Environ. Part A Gen. Topics 25, 207–216.

Wang, T., Ding, A.J., Blake, D.R., Zahorowski, W., Poon, C.N., Li, Y.S., 2003. Chemical characterization of the boundary layer outflow of air pollution to Hong Kong during February–April 2001-art. no. 8787. J. Geophys. Res. Atmos. 108, 8787.

Zhang, X.Y., Wang, Y.Q., Wang, D., Gong, S.L., Arimoto, R., Mao, L.J., Li, J., 2005. Characterization and sources of regional-scale transported carbonaceous and dust aerosols from different pathways in coastal and sandy land areas of China. J. Geophys. Res. Atmos. 110, D15301.

Zhang, X.Y., Wang, Y.Q., Zhang, X.C., Guo, W., Gong, S.L., 2008. Carbonaceous aerosol composition over various regions of China during 2006. J. Geophys. Res. Atmos. 113, D14111.

Zhang, Y.X., Shao, M., Zhang, Y.H., Zeng, L.M., He, L.Y., Zhu, B., Wei, Y.J., Zhu, X.L., 2007. Source profiles of particulate organic matters emitted from cereal straw burnings. J. Environ. Sci. 19, 167–175.

Zhi, G.R., Chen, Y.J., Feng, Y.L., Xiong, S.C., Li, J., Zhang, G., Sheng, G.Y., Fu, J.M., 2008. Emission characteristics of carbonaceous particles from various residential coal-stoves in China. Environ. Sci. Technol. 42, 3310–3315.